

Article

A Fault Location Analysis of Optical Fiber Communication Links in High Altitude Areas

Kehang Xu ^{1,2,*} and Chaowei Yuan ¹

¹ School of Information and Communication Engineering, Beijing University of Posts and Telecommunications, Beijing 100876, China; yuancw2000@bupt.edu.cn

² Southwest Branch of State Grid Corporation of China, Chengdu 610041, China

* Correspondence: kehangxu0419@gmail.com

Abstract: Breakage and damage of fiber optic cable fibers seriously affects the normal operation of fiber optic networks, and it is important to quickly and accurately determine the type and location of faults when they occur. Unlike the old traditional methods, the advantages of wavelet transform in singular signal detection and signal filtering are used to analyze the Optical Time Domain Reflectometer curve signal and the fault detection method of fiber communication links with no relay and a large span in a high altitude area is given, which realizes the accurate detection and location of optical fiber communication link fault events under strong noise. The proposed technology detects fiber optic faults in high-altitude environments, with an average measurement accuracy improvement of 9.8%. The maximum distance for detecting fiber optic line faults is up to 250 km, which increases the system power budget. In the simulation experiment results, the infrastructure nodes of the Wuhan FiberHome Laboratory successfully verified the superiority of this technology. The method has been directly applied to the on-site detection of ultra long optical fiber links in high-altitude areas, which has good financial significance and has certain reference significance for the future real-time detection of optical fiber cables.

Keywords: ultra-low loss fibers; OTDR; wavelet transform; fault detection; high altitude areas



Citation: Xu, K.; Yuan, C. A Fault Location Analysis of Optical Fiber Communication Links in High Altitude Areas. *Electronics* **2023**, *12*, 3728. <https://doi.org/10.3390/electronics12173728>

Academic Editor: Hector E. Nistazakis

Received: 30 July 2023

Revised: 22 August 2023

Accepted: 31 August 2023

Published: 4 September 2023



Copyright: © 2023 by the authors. Licensee MDPI, Basel, Switzerland. This article is an open access article distributed under the terms and conditions of the Creative Commons Attribution (CC BY) license (<https://creativecommons.org/licenses/by/4.0/>).

1. Introduction

Ultra-low-loss (ULL) optical fiber, with a lower transmission loss, more stable transmission performance and excellent long-link transmission capability, is often used in areas with harsh transmission environments, such as sparsely populated areas, uninhabited areas and, especially, at high altitudes. Our research team has studied the fiber loss [1–4] and fiber strength [5,6] under the special environment of high altitude, and found that a change in altitude can have a great impact on the optical fiber splicing point, and also studied the safety of the entire fiber link communication system [7]. Interestingly, there is publicly available classic literature on how to use optical fibers to achieve the application of optical devices [8,9]. In addition, fiber optic performance monitoring tools are a newly proposed technology aimed at efficiently detecting, locating, and estimating fiber optic faults without interrupting data flow, and improving the availability and reliability of fiber optic networks in remote real-time detection of fiber optic faults [10–13]. Moreover, fiber optic sensors can be used to form fiber optic sensing networks (OFSNs), enabling manufacturers to create multifunctional monitoring solutions with multiple applications, such as regular monitoring over long distances (kilometers), or in extreme or hazardous environments, structural and engine interiors, clothing, and health monitoring and assistance [14,15]. However, these classic references have been all implemented in plain areas. More importantly, the stable and reliable operation of the entire optical fiber communication link in high altitude areas needs to be further studied, because the environment is extremely harsh at high altitude and the cost of maintenance is extremely huge. Once the optical fiber link system

is built, it is not desirable to conduct frequent maintenance. It is worth noting that, due to defects and external factors in the manufacturing process of the fiber optic structure itself, the fiber optic line is accidentally damaged, which in turn causes the paralysis of the fiber optic line; by using the failure of the fiber optic line, the interception of fiber optic signals has become increasingly easy and covert, at which point fiber optic communication is no longer safe and reliable [16]. Therefore, it becomes very important to find and recover faults of optical fiber lines early, in order to ensure the smooth flow of optical communication network system.

Currently, the Optical Time Domain Reflectometer (OTDR) is the main measurement instrument used in optical cable line inspection [17–20]. Especially in fiber-optic monitoring systems, OTDR is often used to determine the location of fiber-optic fault points or the fiber length of splice loss [21–26]. J.Z.Christopher has proposed an algorithm to detect and locate fiber faults by digital signal processing of OTDR data by using the method of Gabor series and Rissanen's minimum description length criterion [17–19]; however, the noise in the actual measurement is not very ideal. M.S.Ab-Rahman has proposed and demonstrated a MATLAB-based graphical user interface (GUI) that is capable of measuring optical signal levels, attenuation and locating breakpoints in faulty optical fibers [21], but the theoretical study of this literature lacks in-depth analysis. J.P.V.D.Weid distinguishes meaningful level shifts from typical signal fluctuations which, in turn, is associated with the problem of identifying small losses in noisy OTDR profiles [22], but this method can not average out the noise by increasing the acquisition period. K.Abdelli detects, locates, and estimates the fault of optical fiber by extracting signals from monitoring data obtained by OTDR, which is commonly used for fault diagnosis of fiber links [25,26], but this method is mainly used in the case of high signal-to-noise ratios and takes longer time under the case of low signal-to-noise ratios. In particular, all of these studies do not consider the application scenarios of non-relay, large span ultra-long optical fiber links, especially at high altitudes.

This paper discusses the principles and key techniques of OTDR curve and fault location, and analyzes OTDR signals theoretically by using a wavelet transform, and finally realizes noise reduction and singularity location of OTDR data generated on actual fiber optic lines through simulation. The real-time detection of long-span, relay-free and ultra-long fiber link communications at high altitudes is carried out, and a large amount of field test data are collected. When detecting fiber optic faults in high-altitude environments, the proposed technology enables the maximum distance for detecting fiber optic line faults to reach 250 km, and improves the average measurement accuracy by 9.8%, thereby increasing system power budget. The method has been directly applied to the on-site detection of relay-free, large-span and ultra-long fiber links at high altitudes, which has certain significance for ensuring the reliable operation and real-time monitoring of fiber communication links in the future, with good financial significance.

2. Materials and Methods

OTDR curve analysis is a very important part of fiber remote fault diagnosis. In 1976, Barnoski explained the potential application of optical backscattering in optical measurements [27], and OTDR was developed on this basis. OTDR is a precision optoelectronic integrated instrument made by using the Rayleigh scattering and backscattering generated by Fresnel reflection of optical signals during transmission in optical fibers. This instrument is mainly used for fault monitoring of fiber optic communication links, and is an indispensable instrument for fiber communication technology [28].

Under ideal conditions, OTDR can accurately measure the characteristics of fibers. However, due to equipment accuracy and other reasons, the OTDR curve signal contains a large noise component, especially at the tail end of the curve. Interestingly, its working principle is similar to that of a radar. A pulse light signal is injected into the measured fiber, and when these signals encounter the fusion points, connectors, bends, fractures or the ends of the fiber, some of them are scattered and reflected back into the OTDR [29]. The useful information returned is measured by the optical detector of OTDR, and is used as segments

at different locations within the fiber. The fiber characteristics are determined by analyzing these reflected-back optical signals. The OTDR consists of light source, directional coupler, light detector, sampling analyzer and oscilloscope [30], as shown in Figure 1. Among them, there are many kinds of couplers, but there are two main points in terms of its role: the first is to transmit and couple the light pulses (electro-optic conversion) generated by the light source into the optical fiber to be detected, while transmitting the back reflection and scattered light generated in the optical fiber to the detector; the second is to eliminate the strong Fresnel reflection on the front-end face of the fiber to be tested. A photodetector is a device that receives back-facing light signals and outputs them as electrical signals.

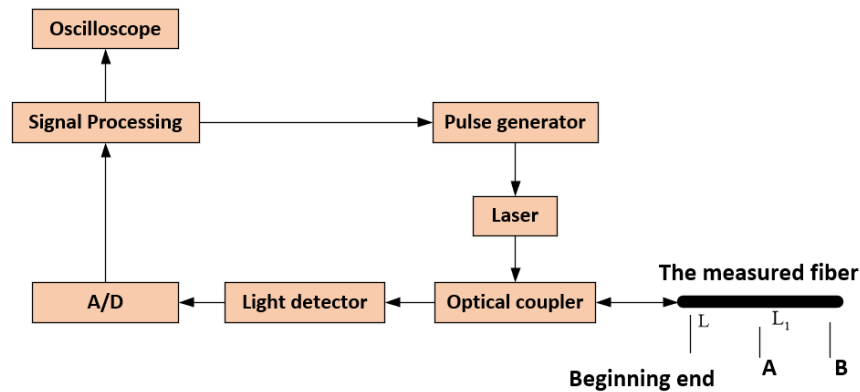


Figure 1. Structure diagram of OTDR.

OTDR uses Rayleigh scattering and Fresnel reflection to characterize optical properties [30,31]. When light is transmitted in an optical fiber, Rayleigh scattering is caused by the slight fluctuation of the refractive index of fiber, while Fresnel reflection is caused by the abrupt change in the refractive index at the end face or fault point of fiber, which is a discrete reflection. Notably, Rayleigh scattering is determined by the properties of the fiber material itself, while Fresnel reflection is related to the actual operation and state of each fiber, and reflects the “point” event on the fiber.

The Rayleigh scattering signal generated by OTDR is a slow downward decaying curve that decreases as the laser beam travels a greater distance through fiber. According to scattering principle, the optical power of Rayleigh backscattering is proportional to the pulse width of the incident laser beam when the signal wavelength is determined. Especially, the longer the pulse width is, the stronger the Rayleigh backscattering becomes. The power reflected from the fiber, namely, the Rayleigh backscattered light power obtained by the OTDR optical receiver, P_{rs} , can be calculated by Equation (1).

$$P_{rs}(L) = \frac{1}{2} S c \alpha_s \tau P_0 \exp(-2\alpha L). \tag{1}$$

where $L = V_f t / 2$ represents distance from the fiber injection end; c represents speed of light in vacuum; V_f represents propagation speed of light in fiber; P_0 represents the pulse power at the injection end of the optical fiber at $t = 0$, namely, the peak power of the optical pulse injected into optical fiber; $\tau = l_p / V_f$ represents incident laser pulse width; l_p represents pulse space; $\alpha_s = 2P_{TS} / l_p P_0$ represents Rayleigh scattering attenuation coefficient; P_{TS} represents total Rayleigh scattering power; α represents attenuation coefficient of fiber; and S represents the ratio of back Rayleigh scattering power to total Rayleigh scattering power, also called the backscattering coefficient. For a single-mode fiber,

$$S_{sm} = \frac{3/2}{(\omega_0/r)^2 V^2} \left(\frac{NA}{n_1} \right)^2. \tag{2}$$

where $NA = \sqrt{n_1^2 - n_2^2}$ represents the numerical aperture of optical fiber; n_1 and n_2 are the refractive index of the core and cladding, respectively; r represents fiber core radius;

and ω_0 represents spot size. In addition, the normalized frequency V is a fiber structure parameter proportional to the optical wave frequency and can be expressed as Equation (3).

$$V = k_0 r \sqrt{n_1^2 - n_2^2}. \quad (3)$$

where $k_0 = 2\pi/\lambda$ represents phase constant and λ is the operating wavelength.

Fresnel reflection is caused by individual points in the whole fiber. It is worth noting that these points can occur at any joint point in the fiber, where there is serious geometric distortion or where the fiber is broken or disconnected. At this time, the change in the backscattering coefficient due to the change in the refractive index can generate strong backscattered light. OTDR captures these optical signals and uses them to determine the fault point, breakpoint and other information of the optical fiber. Especially, the width of the laser pulse injected into the fiber from OTDR is adjustable, and the period of the OTDR emission pulse can be calculated [30], as shown in Equation (4).

$$t = 2 \frac{Ln}{c}. \quad (4)$$

where t represents total time from the signal transmitter to the receiver and n represents the specified refractive index.

Let the power reflection coefficient of the optical fiber be β_f . Then, the power returned from the optical fiber, namely, the Fresnel reflected light power obtained by OTDR optical receiver, P_{fr} , can be calculated by Equation (5).

$$P_{fr}(L) = \beta_f P_0 \exp(-2\alpha L). \quad (5)$$

From Equations (1) and (5), both Rayleigh scattered power and Fresnel reflected power are proportional to their backscattering coefficients and inversely exponential to their attenuation coefficients. Moreover, the smaller the backscattering coefficient is, the smaller the reflected power becomes and, conversely, the larger the reflected power becomes. In addition, it can be seen from Equation (2) that the backscattering coefficient of a single-mode optical fiber is, in turn, inversely proportional to the core diameter, spot size and operating wavelength of the optical fiber.

Singularities, irregular and abrupt parts of the signal, often carry more important information. The Fourier transform has been one of the most widely used tools in the field of signal processing. Unfortunately, the analysis of non-smooth signals based on the Fourier transform cannot provide complete information. Wavelet transform (WT) inherits and develops the idea of Fourier transform localization, overcoming the disadvantages of the window size not being able to vary with the frequency. It has good localization characteristics and the advantages of both time and frequency domain analysis, and can thus focus on any details of the signal object.

Let $\psi(t)$ be a square integrable function, namely $\psi(t) \in L^2(\mathbb{R})$, if its Fourier transform $\Psi(\omega)$ satisfies:

$$C_\Psi = \int_{\mathbb{R}} \frac{|\Psi(\omega)|^2}{|\omega|} d\omega < \infty. \quad (6)$$

then $\psi(t)$ is said to be a permissible wavelet and Equation (6) is said to be the permissible condition of the wavelet function. Analyzing the inner product of the wavelet function and the signal $x(t)$, the time domain expression of the wavelet transform can be obtained, as expressed in Equation (7).

$$WTx(a, \tau) = \frac{1}{\sqrt{a}} \int_{-\infty}^{+\infty} x(t) \psi\left(\frac{t-\tau}{a}\right) dt. \quad (7)$$

Meanwhile, the frequency domain of wavelet transform equivalent can be expressed by Equation (8).

$$WTx(a, \tau) = \frac{\sqrt{a}}{2\pi} \int_{-\infty}^{+\infty} X(\omega) \Psi(a\omega) e^{j\omega\tau} d\omega. \quad (8)$$

where $x(t)$ represents the signal to be analyzed, and $X(\omega)$ and $\Psi(\omega)$ are the Fourier transforms of $x(t)$ and $\psi(t)$, respectively. By properly selecting the basis wavelet, it is possible to have limited support for $\psi(t)$ in the time domain, and it is also more concentrated in the frequency domain. In other words, WT can show the local features of the signal in both time domain and frequency domain, which is very beneficial to detect transient signals or singularities.

Mutation signals are divided into edge-hopping and peak-hopping. In signal analysis, mutant signals have singularity at mutation point. The signal singularity can be detected from the modal maxima of its wavelet transform [32]. In a few words, under the scale 2^j , in a certain neighborhood δ of t_0 , for any t , it satisfies:

$$|W_{2^j}f(t)| \leq |W_{2^j}f(t_0)|. \quad (9)$$

The point t_0 is the modal extremum of the wavelet transform. Especially, it is still the modal extremum of the wavelet transform at $W_{2^j}f(t_0)$.

In a fiber optic fault diagnosis system, we mainly focus on the location and the type of the fault so that we can restore the optical communication operation in time. A strong light narrow pulse is injected into the input end of the measured optical fiber. Due to the actual nonuniformity inside the optical fiber, the light can be scattered along each point of the optical fiber when it is transmitted inside the optical fiber, and then the scattered light can return to the incident end of the optical fiber in the direction opposite to the incident light in the optical fiber. Because the main scattering mechanism is Rayleigh scattering, the detection of the backscattered light power at each point along the length of the optical fiber all contains the information of the loss of light in the optical fiber transmission. Therefore, the loss characteristics and defect points of the optical fiber can be analyzed and judged.

Generally speaking, the events on the OTDR test curve can be divided into blind spots, non reflection events, reflection events and optical fiber terminals, as shown in Figure 2. It is worth noting that the farther the long-distance optical fiber is from the detection position, the easier it is to present different states. This is because, in addition to the fiber fault itself, it is also affected by the external environment, which leads to more complex bending and winding on the OTDR curve.

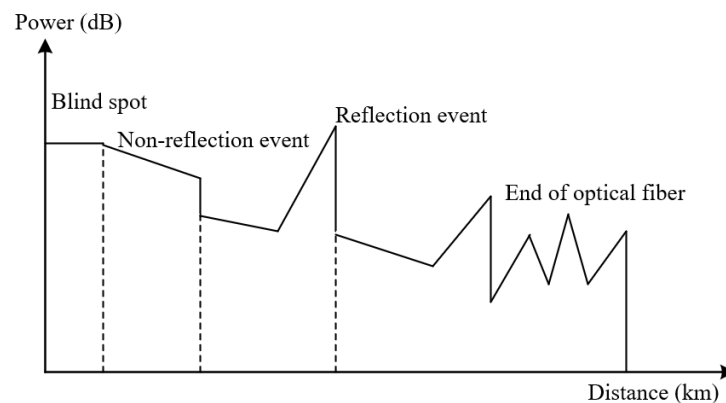


Figure 2. OTDR event types.

In order to accurately detect events, the noise is sufficiently suppressed while highlighting useful information. We first perform wavelet transform on the OTDR curve data, and then perform threshold filtering on the high-frequency information, and finally perform energy operation, since the mutation information exists in the high-frequency information after wavelet decomposition, as shown in Figure 3. Furthermore, the event information is

retained in the curve and enhanced, while the noise in the curve is sufficiently suppressed, which is very beneficial for the detection of the event points. Fortunately, the location of an event point is accurately examined by the event detection algorithm [33].

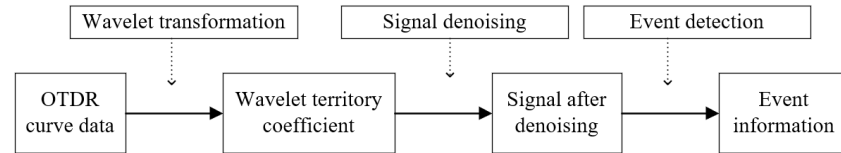


Figure 3. Event detection process.

Due to equipment accuracy and other reasons, the OTDR curve signal contains a large noise component, especially at the tail part of the curve. Therefore, it is very necessary to perform noise reduction on the curve before curve analysis, as well as fault location and diagnosis. Further, the curve data is displayed digitally and analyzed based on the assumptions of the parameters of the tracking analysis of the curve. Then, certain event points are identified on the curve. Consequently, the operating status of the fiber is obtained.

The actual signal measurement process generally introduces noise. The OTDR detected data is a linear combination of the original data and noise. Coincidentally, WT is a linear transform, so the WT value of detected data is also superimposed from that of original data and that of noise. Therefore, WT mode maxima can be generated by the test noise. For the actual signal, the WT mode maxima can test its singularity to determine the occurrence time and recovery time of the event when the background noise signal is strong. However, there can be a large error at this time. In order to reduce the impact of the error, the signal can be denoised, both to eliminate the noise after the display of high-frequency quantities, and also to retain some of these high-frequency quantities in response to sudden changes in signal.

According to the attenuation characteristics of optical fiber communication, the OTDR signal containing noise can be expressed as Equation (10).

$$s(t) = f(t) + \sigma \times n(t). \tag{10}$$

where $f(t)$ represents the true signal; $n(t)$ represents the noise signal; $s(t)$ represents the signal containing noise; and σ represents a wavelet function. Special attention can be paid to the preservation of useful signals and recovery of the true signal $f(t)$ from $s(t)$ when noise reduction is applied to the $s(t)$ signal, since the OTDR curve event points are high-frequency signals.

Here, the signal-to-noise ratio (SNR) is used to measure the effect of OTDR curve signal noise reduction, which can be calculated by Equation (11).

$$SNR = 10 \times \log_{10} \left(\frac{P_s}{P_n} \right). \tag{11}$$

where P_s represents the real signal power and P_n represents the noise power. They can be shown by Equation (12) and Equation (13), respectively.

$$P_s = \frac{1}{n} \sum_{i=1}^n f^2(i). \tag{12}$$

and

$$P_n = \frac{1}{N} \sum_{n=1}^N [f(n) - f'(n)]^2. \tag{13}$$

where $f(n)$ represents the original signal; $f'(n)$ represents the signal after wavelet noise reduction; and N represents the sample size.

Except for the low-frequency component, the wavelet coefficients of each component are distributed almost symmetrically on both sides of the zero point [34]. Most small-scale coefficients are small. To keep the major edges, an intuitive and effective way to remove noise is to take a threshold value directly on the wavelet coefficients. Furthermore, only by keeping the larger coefficients can the original signal be reconstructed, since the distribution of the wavelet coefficients is Gaussian normal. Based on WT, a threshold is given as noise standard deviation and N is given as the number of signal sampling points [35]. Unfortunately, this threshold is too large when it is large and too small when it is small. Thus, instead of using the factor $2\log N$, it is usually generated by the constant c , namely $T = c\sigma$, which in turn achieves a “soft threshold” that calculates the absolute value of the wavelet coefficients, as shown by Equation (14). Generally speaking, the optimal c value varies with different signals and noise levels. Experiments have shown that it is reasonable to choose a c value of between 3 and 4 for ordinary signals. Here, $c = 3.452$ is taken.

$$W(i) = \text{sgn}[W(i)] \cdot [|W(i) - T|]_+ \quad (14)$$

The threshold value given here is calculated as $T_m = c\sigma_m$, and in which type, m is the scale; σ_m is the scale with noise variance of m . Generally speaking, the best value for c can vary with the different signals and the noise intensity. Experiments show that it is more appropriate to take c between 3 and 4 for ordinary signals [26,34], and here $c = 3.4641$.

Considering that the curve can be influenced by other factors, we choose the orthogonal wavelet basis with low vanishing moment and small support length to realize the analysis of OTDR curve. Furthermore, we here let the wavelet scale be between 2 and 4 after many trials, since the signal used is the data obtained by noise reduction and, especially, the fiber length of fiber optic cables in high altitude areas is long.

3. Experiment

To date, there are too few and imperfect field experiments for fiber-optic fault detection under the harsh climatic conditions. Additionally, experimental data on fiber-optic faults at high altitudes that can be used for analysis and application are seriously lacking. The standard Corning SMF-28 ULL fiber, which is a “step-type” single-mode fiber, is chosen as the research object. To exclude unnecessary interference and facilitate the calculation, the ULL fibers used in the experiment all are from the same manufacturer, the same batch and the same type. The material parameters and geometric parameters of ULL fibers all are taken as their average values, as shown in Table 1.

Table 1. Characteristic parameters of optical fiber.

ULL	r (μm)	D (μm)	MFD (μm)
average value	4.3125	125.1216	10.257

When using the EXFO MAX-730B-M2 OTDR testing, it is necessary to first set the instrument parameters, among which the most important is to set the refractive index and testing wavelength of the testing fiber. Only when the basic parameters of the test instrument are accurately set can the conditions be created for accurate testing. We build the optical fiber fault detection device in high altitude areas after the basic indicators and their parameters are set, as shown in Figure 4.

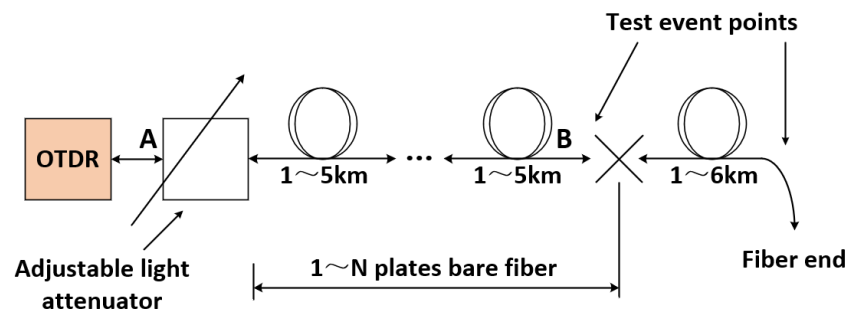


Figure 4. Optical fiber fault test device.

Here, point *B* is placed at the measured event point, which can be the fusion point or fiber segment with a loss of 0.5 dB; *A* is adjustable attenuator. During the period, we gradually increase the adjustable attenuator until the measurement results of the measured event point relying on OTDR deviate from the true value, and at which point the attenuation between *A* and *B* is recorded.

Accurate and complete fiber line data are the basic basis for fault measurement and location. Based on China's "Tibet-Central" networking project, we select two optical fiber lines in "Mozhu-Lhasa" as the detection object. In order to exclude the interference of the fiber itself, 10 samples are taken for each selected experiment and the samples, and their parameters are assumed to be consistent in the same sample space. In addition, the test range selected here is controlled to be about 1.25 times of the fiber length.

4. Results and Discussion

"Slope" is common in OTDR signals, which indicates clearly that there is loss at this place. There are many reasons for this phenomenon, such as joint defects. As described in the second part of the article, there are two different backscatter signal waveforms when OTDR is used to detect optical fiber link faults. Figure 5 shows the real OTDR field test curve, where the x-axis variable represents "distance" and the right axis with blue numbers represents "return loss". Among them, the waveform shown in Figure 5a has a strong Fresnel reflection peak and a very large negative step, which indicates that the optical fiber has a good termination at this fiber failure. Especially, the waveform shown in Figure 5c has only one negative step, which indicates that the fiber link of the cable is crushed or broken at that location. By contrast, the fiber optic communication link shown in Figure 5b is in good condition. In addition, Figure 5a also shows that the signal after the negative step continues to be transmitted at low power. Namely, the OTDR receiving end still receives optical signals at this time, but it is lower than normal value, which implies the fault point is at the negative step. Figure 5c also shows that the fiber link from point *A* to point *B* in Figures 1 and 4 is a fault section. There are many reasons for bringing errors to the accuracy of OTDR measurement. We assume that the OTDR equipment parameters have been well adjusted when analyzing the OTDR curve signal, which helps to evaluate the safe operation of optical fiber link communication. In brief, the proposed fault detection method can accurately detect the operating status of optical fiber cables. Once a fault is detected in a certain section of optical fiber, an early warning will occur, so that the maintainer can make a correct choice in the first time to carry out rapid maintenance, thereby minimizing the signal stagnation time and reducing the probability of optical information packet loss. Ultimately, the reliability and efficiency of optical communication system in high altitude area are improved.

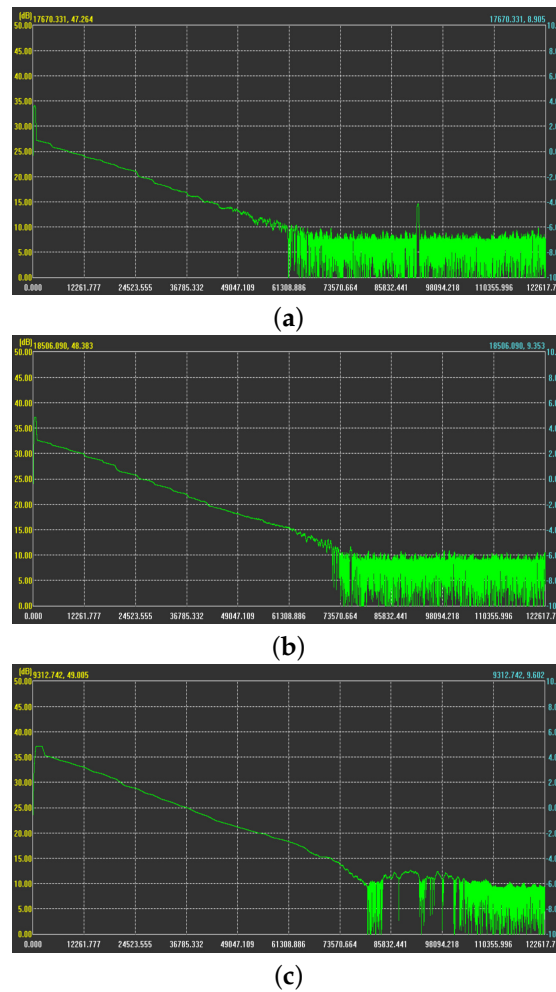


Figure 5. OTDR test curve, (a): minor fault; (b): normal; (c): serious fault.

According to the second part of this paper, OTDR collects and quantifies the returned backscatter signal on the basis of the return time, area difference and optical power variation in a sample, and then displays the measured fiber backscatter curve in the geometric plane on the oscilloscope. The main role of OTDR is to measure the performance of fiber and to determine the location of the failure point of the fiber. As shown in Figure 5, certain irregular singularities and abrupt changes in the OTDR curve signal contain some important information. We analyze the OTDR curve using WT according to its advantages in singular signal detection and signal filtering and combine it with Equation (14) to achieve accurate detection and localization of fault events under strong noise. Simulation results are shown in Figure 6. When the signal encounters a fault or fiber break, a sharp reflected signal is superimposed on the backward scattering signal, and the backward scattering curve reacting to original data has a large abrupt change at this time. The actual operation effect shows that, using WT, the accuracy and precision of fiber fault location have been improved in performance, and the effect is remarkable, which also verifies the method in this paper from the side, i.e., the wavelet threshold denoising method can effectively improve the accuracy of OTDR curve analysis.

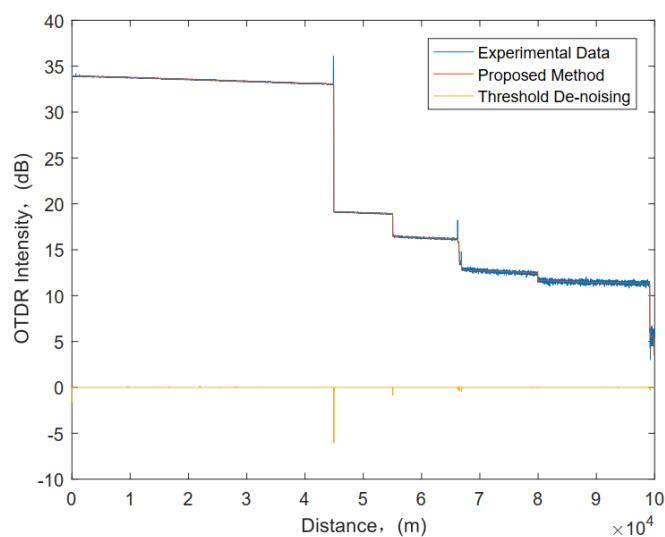


Figure 6. OTDR intensity vs. distance.

There are numerous reasons for fiber link failure, including fiber deformation due to external forces on the fiber, inadequate performance of the fiber itself, connector failure and external causes. To facilitate the analysis, we describe the fiber profile status of OTDR testing as event types containing blind spot, non-reflective event, reflective event and the end. According to the second part of this paper, the magnitude of the optical signal power can characterize advantages and disadvantages of transmission characteristics of the fiber optic cable line. The obtained amplitude of the optical power transformation is different for different fault conditions. Depending on the severity of the fault, the power can range from normal values to zero. Combined with Equations (1), (4) and (5), we obtain the change trend of the power of different events transmitted along the fiber link, as shown in Figure 7. The power gradually decreases with the increase in the transmission distance of signal. However, when the optical signal propagation occurs in a special state, reflection and other situations can occur, and the power can also change accordingly at this time. That the obtained power is smaller than the normal value indicates that the attenuation of the optical fiber link is increasing. Furthermore, that the optical power at the receiving end is zero indicates that the transmission distance of the optical signal has reached its limit, or that a complete interruption of the fiber has occurred, namely the highest level of failure. Specially, we can also record the time taken for optical signal to return from the transmission signal, and then determine propagation speed of optical signal in the fiber medium, and thus calculate the distance. Notably, it is the first time for us to conduct research on fiber optic cable fault detection in high-altitude areas. Additionally, the environment in high-altitude areas is extremely harsh, so it is difficult for us to obtain data during the experiment. However, the obtained data can well reflect the current operating status of the fiber optic link at that time. In other words, in terms of correctly identifying and locating optical fiber optic cable operational faults, the method proposed achieves the expected accuracy and success rate.

In the actual engineering, the useful curve signal is usually shown as some low frequency signal, relatively smooth signal or singularity signal, while the noise signal is usually the high frequency signal. It is worth noting that OTDR curve event points are typically high-frequency signals, so special attention can be paid to the retention of the useful signal during signal noise reduction, which is very beneficial to the subsequent recovery of the real optical signal from it. In conjunction with Figures 5 and 6, we can decompose the original noisy signal under scale 3 to obtain the noise reduction threshold, and then use the soft threshold method to process and reconstruct the OTDR curve signal, as shown in Figure 8. Obviously, although the OTDR signal is disturbed by strong noise, we can clearly see that the noise is effectively suppressed after threshold denoising of each

wavelet domain coefficient. In particular, the discontinuity marks and positions of the signal points correspond well.

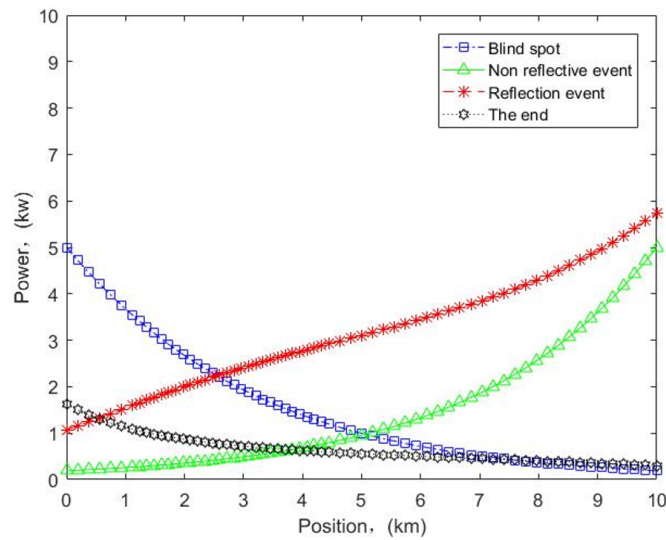


Figure 7. Power vs. event location.

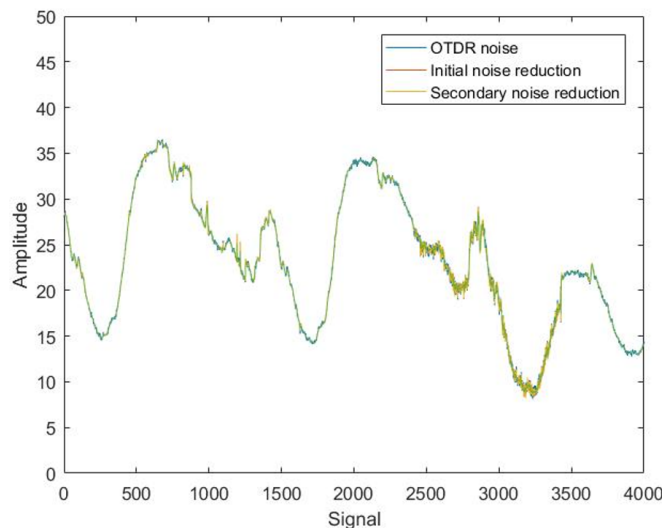


Figure 8. Threshold noise reduction, amplitude vs. signal transmission distance.

The OTDR curve signals are actually the Fresnel reflection, jump or other events, which all belong to the first type of discontinuity. In short, the signal changes suddenly at a certain time. Then, it can be judged by using a base wavelet having a first-order vanishing moment. Based on Figures 6 and 8, the processing speed and time requirements of equipment hardware is considered to improve the accuracy. Then, we introduce the signal-to-noise ratio. Then, based on Equations (10)–(13), we analyze the processing effect of this model, as shown in Figure 9. Apparently, the SNR for the 10 sample points obtained are not consistent and vary widely. Notably, the SNR after denoising all have been increased evidently. Namely, the noise reduction effect is fine here. In addition, the average value of SNR obtained has reached 43.6911 dB, which has satisfied the demand. In particular, a larger SNR obtained indicates that the signal is the main component and the decomposition scale can be appropriately tuned down. On the contrary, the decomposition scale can be appropriately tuned up. Notably, it is difficult for us to stay for a long time to obtain a large number of experimental data, because the environment in the high-altitude area is extremely harsh. We can only collect data around July and August of the year, and it makes sense that this is meaningful enough to meet the needs of high-altitude power communication cable

fiber optic lines rolling out smoothly. It is of great practical significance, which once again supports the effectiveness of the research results in this paper from a lateral perspective.

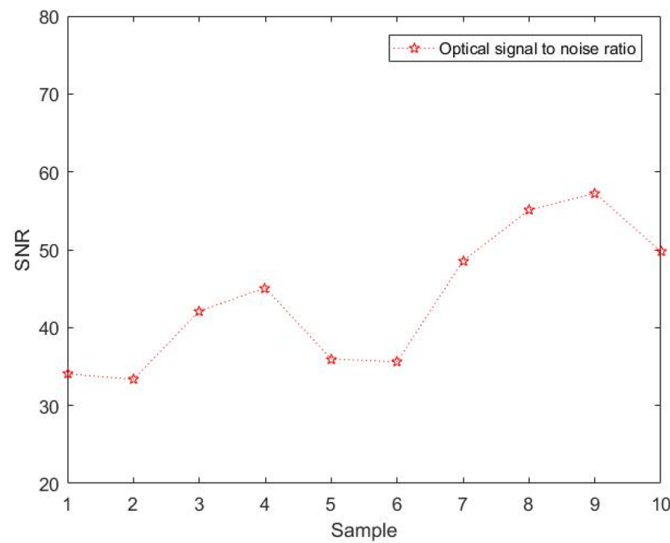


Figure 9. Signal-to-noise ratio vs. sample.

To verify the accuracy of the proposed model, we have conducted field tests at high altitudes and obtained a large amount of experimental data. Combined with the second part of this paper and Figures 5 and 7, the simulation results of the curve test events of OTDR are shown in Figure 10. Obviously, the non-reflection events are relatively smooth, which indicates normal transmission of the optical signal, while the blind spot occasionally changes abruptly, which indicates increased reflection at this time and can seriously affect the accuracy of fiber length measurements. In particular, although the reflection event is not regular and contains Rayleigh scattering and Fresnel reflection, it is the core of fiber fault location detection. Here, the detection location and event type of events basically match with the actual situation, with high accuracy. Notably, the longer the optical fiber is, the lower the accuracy of the fault detection method becomes, because at this time, the farther the optical fiber segment from the detection device is, the more likely it is to be affected by other uncontrollable factors. In addition, the stronger the signal, the more able it is to detect the operating status of the optical fiber. In other words, the higher the signal strength is, the more accurate the fiber optic cable detection method becomes.

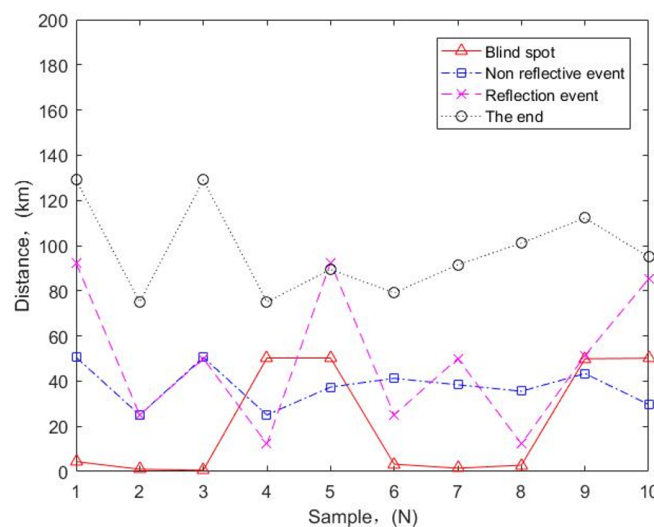


Figure 10. Optical fiber distance vs. event sample.

To further verify the accuracy of the model, we examine Figure 10 for further analysis of reflection events and obtain corresponding curves, as shown in Figure 11. Obviously, despite the large fluctuations of the reflected events, there is not much deviation for each reflected event point, which indicates that the positions of checked reflected events basically match the positions of the actual reflected events, which again verifies the high accuracy of the model proposed. It is worth noting that, although there is no regularity in the detection of reflection events, it does not affect application of the method proposed to the event detection of large span, unrepeated fiber optic links at high altitudes. For example, if the fault point is observed through OTDR curve, there is an obvious Fresnel reflection peak. Then, compared with the data, if the distance from a certain joint is close, it can be preliminarily judged as an optical fiber fault in the box. Furthermore, if the distance between the fault point and the joint is large, it is a fault in the cable. It is worth noting that this article has combined the OTDR technology with wavelet transform to improve the accuracy of long-distance fiber fault location in a high-altitude environment for the first time, filling the technical gap in the field of optical fiber fault diagnosis in harsh environments, and expanding the fiber fault database.

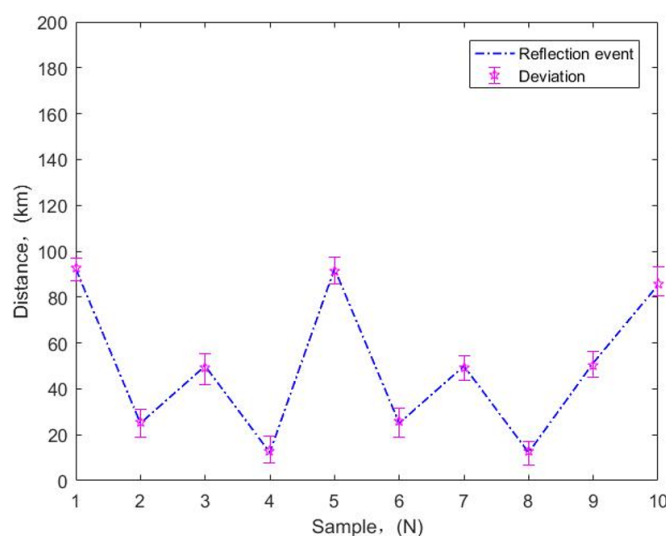


Figure 11. Optical fiber distance vs. Reflection event sample.

5. Conclusions

Here, WT is introduced into the fiber fault diagnosis system. The OTDR signal is analyzed and the noise reduction and singularity location of OTDR data generated on the actual fiber line are realized through simulation. The fault detection method of relay-free and large-span optical fiber link communications in high altitude areas is given. A large amount of the field test data is collected. Especially, the results obtained using OTDR technology are intuitive and very easy to analyze. In addition, existing methods used in fiber optic fault diagnosis systems are very effective in plain areas, but in the high-altitude environments, they either fail or have very low accuracy. The method here has achieved significant results in practical fiber optic cable engineering in high-altitude areas, as well as in terms of accuracy improvement. The infrastructure nodes of Wuhan Fenghuo Laboratory have successfully verified the superiority of the technology in this article. The average measurement accuracy of detecting fiber optic faults in high-altitude environments has been improved by 9.8%, and the maximum distance for detecting fiber optic line faults can reach up to 250 km, increasing the system power budget. How to choose threshold value and how to perform threshold quantization all have a great impact on the quality of signal noise reduction. The method proposed has been directly applied to the field detection of non-relay and long-span ultra-long optical fiber optic links in high altitude areas, achieving good results and greatly reducing economic costs, which has certain reference significance.

for ensuring the reliable operation and real-time monitoring of fiber optic communication links in the future.

Author Contributions: Conceptualization, K.X.; Methodology, K.X.; Formal analysis, K.X.; Investigation, K.X.; Writing—original draft, K.X.; Writing—review & editing, K.X.; Supervision, C.Y. All authors have read and agreed to the published version of the manuscript.

Funding: This work is supported by the Science and Technology Project of State Grid Corporation of China (SGLNDK00KJJS1700200); the National Key Research and Development Program of China (2020YFB1807901).

Data Availability Statement: Not applicable.

Acknowledgments: All authors would like to thank the editor and the reviewers for their reviews and suggestions to help us improve the quality of this paper.

Conflicts of Interest: We declare that we have no financial and personal relationships with other people or organizations that can inappropriately influence our work reported in this manuscript, and there is no professional or other personal interest of any nature or kind in any product, service and/or company that could be construed as influencing the content presented in, or the review of, the manuscript entitled.

References

1. Cui, Z.; Yuan, C.; Xu, K.; Sun, Y.; Yin, S. Modeling the splice loss of single-mode optical fibers affected by altitude. *IEEE Access* **2019**, *7*, 99283–99289. [\[CrossRef\]](#)
2. Cui, Z.; Yuan, C. The effect of fusion current on thermally diffused expanded core of splicing ultra-low loss fiber and traditional single-mode fiber. *Opt. Fiber Technol.* **2021**, *63*, 102477. [\[CrossRef\]](#)
3. Cui, Z.; Yuan, C.; Li, C. Modeling the splice loss of ultra-low loss fiber and single-mode optical fiber in high altitude area. *Opt. Fiber Technol.* **2021**, *67*, 102696. [\[CrossRef\]](#)
4. Hu, L.W.; Yuan, C. Analysis of Splice Loss of Single-Mode Optical Fiber in the High Altitude Environment. *Coatings* **2021**, *11*, 876. [\[CrossRef\]](#)
5. Hu, L.W.; Yuan, C.W. Modeling and analysis of the fusion strength of single-mode optical fiber in the high altitude environment. *Opt. Mater. Express* **2022**, *12*, 2995–3014. [\[CrossRef\]](#)
6. Hu, L.W.; Yuan, C. Improvement in fusion performance between G652.D fiber and Ultra-low-loss fiber by controlling discharge current of fusion splicer. *Opt. Fiber Technol.* **2023**, *79*, 103368. [\[CrossRef\]](#)
7. Xu, K.H.; Li, X.; Tang, Y.; Yuan, C. Serial-parallel combined all optical sequence matching system using highly nonlinear fibers for photonic firewall. *Optik* **2021**, *244*, 167571. [\[CrossRef\]](#)
8. Pinhas, H.; Malka, D.; Danan, Y. Design of fiber-integrated tunable thermo-optic C-band filter based on coated silicon slab. *J. Eur. Opt. Soc.-Rapid Publ.* **2017**, *13*, 32. [\[CrossRef\]](#)
9. Gelkop, B.; Aichnboim, L.; Malka, D. RGB wavelength multiplexer based on polycarbonate multicore polymer optical fiber. *Opt. Fiber Technol.* **2021**, *61*, 102441. 2020.102441. [\[CrossRef\]](#)
10. Ahmed, A.I.; Mohammed, M.F.; Azhar, A.H. A Design Fiber Performance Monitoring Tool (FPMT) for Online Remote Fiber Line Performance Detection. *Electronics* **2022**, *11*, 3627.
11. Ahmed, A.I.; Mohammed, M.F.; Azhar, A.H. Remote Real-Time Optical Layers Performance Monitoring Using a Modern FPMT Technique Integrated with an EDFA Optical Amplifier. *Electronics* **2023**, *12*, 601.
12. Elsayed, E.E.; Yosif, B. Performance evaluation and enhancement of the modified OOK based IM/DD techniques for hybrid fiber/FSO communication over WDM-PON systems. *Opt. Quantum Electron.* **2020**, *52*, 385. [\[CrossRef\]](#)
13. Elsayed, E.E.; Yousif, B.B.; Singh, M. Performance enhancement of hybrid fiber wavelength division multiplexing passive optical network FSO systems using M-ary DPPM techniques under interchannel crosstalk and atmospheric turbulence. *Opt. Quantum Electron.* **2022**, *54*, 116. [\[CrossRef\]](#)
14. Pendão, C.; Silva, I. Optical Fiber Sensors and Sensing Networks: Overview of the Main Principles and Applications. *Sensors* **2022**, *22*, 7554. [\[CrossRef\]](#) [\[PubMed\]](#)
15. Li, P. Fault Prediction Analysis of Communication Optical Fiber Based on SVM Algorithm. International Conference on Artificial Intelligence for Communications and Networks. *Artif. Intell. Commun. Netw. AICON* **2021**, *396*, 82–86.
16. Mouftah, H.T. *Optical Networks Architecture and Survivability*; Kluwer Academic: Norwell, MA, USA, 2003; pp. 70–110.
17. Zarowski, C.J. Connection splice fault location in fibre optic cables. In Proceedings of the Conference on Electrical & Computer Engineering, Calgary, AB, Canada, 26–29 May 1996; IEEE: New York, NY, USA, 1996.
18. Liu, F.; Zarowski, C.J. Detection and Estimation of Connection Splice Events in Fiber Optics Given Noisy OTDR Data-Part I: GSR/MDL Method. *IEEE Trans. Instrum. Meas.* **2001**, *53*, 546–556. [\[CrossRef\]](#)
19. Liu, F.; Zarowski, C.J. Detection and location of connection splice events in fiber optics given noisy OTDR data. Part II. R1MSDE method. *IEEE Trans. Instrum. Meas.* **2004**, *53*, 546–556. [\[CrossRef\]](#)

20. Liu, F.L.; Zarowski, C.J. Detection and estimation of connection splice events in fiber optics given noisy OTDR data. *IEEE Trans. Instrum. Meas.* **2001**, *50*, 47–58.
21. Ab-Rahman, M.S.; Chuan, N.B.; Premadi, A. A new approach for identifying fiber fault and detecting failure location. In Proceedings of the International Conference on Electronic Design, Penang, Malaysia, 1–3 December 2008; IEEE: New York, NY, USA, 2009.
22. von der Weid, J.P.; Souto, M.H.; Garcia, J.D.; Amaral, G.C. Adaptive Filter for Automatic Identification of Multiple Faults in a Noisy OTDR Profile. *J. Light. Technol.* **2016**, *34*, 3418–3424. [[CrossRef](#)]
23. Zhu, M.; Zhang, J.; Wang, D.; Sun, X. Optimal Fiber Link Fault Decision for Optical 2D Coding Monitoring Scheme in Passive Optical Networks. *J. Opt. Commun. Netw.* **2016**, *8*, 137–147. [[CrossRef](#)]
24. Nakamura, A.; Okamoto, K.; Koshikiya, Y.; Manabe, T. Potential Fault Detection in Optical Cables Using OTDR Operating in Two-Modes. In Proceedings of the 2019 24th OptoElectronics and Communications Conference (OECC) and 2019 International Conference on Photonics in Switching and Computing (PSC), Fukuoka, Japan, 7–11 July 2019.
25. Abdelli, K.; Griesser, H.; Ehrle, P. Reflective Fiber Faults Detection and Characterization Using Long-Short-Term Memory. *arXiv* **2022**, arXiv:2204.07058.
26. Abdelli, K.; Griesser, H.; Tropschug, C. Optical Fiber Fault Detection and Localization in a Noisy OTDR Trace Based on Denoising Convolutional Autoencoder and Bidirectional Long Short-Term Memory. *J. Light. Technol.* **2022**, *40*, 2254–2264. [[CrossRef](#)]
27. Barnoski, M.K.; Jensen, S.M. Fiber waveguides: A novel technique for investigating attenuation characteristics. *Appl. Opt.* **1976**, *15*, 2112–2115. [[CrossRef](#)] [[PubMed](#)]
28. Keiser, C. *Optical Fiber Communication*, 3rd ed.; Electronic Industry Press: Beijing, China, 2005.
29. Tang, L.; Qi, B.; Chen, C.H.; Zhang, G.-B. Wavelet transform based algorithm for optical fiber fault analysis. *Proc. Chin. Soc. Electr. Eng.* **2006**, *26*, 101–105.
30. King, J.P.; Smith, D.F.; Richards, K.; Timson, P.; Epworth, R.; Wright, S. Development of coherent OTDR instrument. *J. Light. Technol.* **1987**, *5*, 616–624. [[CrossRef](#)]
31. Philen, D.L.; White, I.A.; Kuhl, J.F. Single-mode fiber OTDR: Experiment and theory. *Quantum Electron.* **1982**, *18*, 1499–1508. [[CrossRef](#)]
32. Mallat, S.; Hwang, W.L. Singularity detection and processing with wavelets. *IEEE Trans. Inf. Theory* **1992**, *38*, 617–643. [[CrossRef](#)]
33. Selvarajan, A. *Optical Fiber Communication Principles and Systems*; McGraw-Hill: New York, NY, USA, 2003; pp. 102–126.
34. Zhu, L. The study of OTDR event analysis algorithm base on Wavelet Transform. *Mod. Electron. Tech.* **2004**, *27*, 106–108.
35. Ma, S. The application of haar wavelet and the least squares method in fiber optic monitoring system. *Railw. Comput. Appl.* **2007**, *16*, 32–35.

Disclaimer/Publisher’s Note: The statements, opinions and data contained in all publications are solely those of the individual author(s) and contributor(s) and not of MDPI and/or the editor(s). MDPI and/or the editor(s) disclaim responsibility for any injury to people or property resulting from any ideas, methods, instructions or products referred to in the content.